Unified Model of Switching and Nonswitching Charge-Density-Wave Dynamics

Jeremy Levy and Mark S. Sherwin
Physics Department and Center for Nonlinear Science, University of California, Santa Barbara, California 93106-9530

Farid F. Abraham[a]
IBM Almaden Research Center, 650 Harry Road, San Jose, California 95120-6099

Kurt Wiesenfeld
School of Physics, Georgia Institute of Technology, Atlanta, Georgia 30332-0430
(Received 28 January 1992)

We show that the dynamics of both switching and nonswitching charge-density waves can be described by the classical Fukuyama-Lee-Rice model when the effects of normal carriers (present for $T>0$) are properly taken into account. We have constructed a circuit representation of the model and have performed numerical simulations in one dimension. We find switching in the limits of strong pinning or large normal-carrier resistance, consistent with experiment.

PACS numbers: 72.15.Nj, 05.45.+b

The nonlinear dynamics of sliding charge-density waves (CDWs) has been studied extensively in the past fifteen years [1]. Two classes of CDW behavior have been observed experimentally. Conventional, or "nonswitching," behavior is characterized by a smooth, nonhysteretic I-V curve and a unique threshold field for sliding. Much of the nonswitching behavior is well described by the Fukuyama-Lee-Rice (FLR) model [2,3], which treats the CDW phase as a classical field and ignores amplitude fluctuations of the CDW order parameter.

So-called "switching" behavior [4] is characterized by an abrupt, hysteretic transition into the sliding state. Switching was first observed in $NbSe_3$, and subsequently in other materials such as TaS_3, $(NbSe_4)_{3.33}I$, $K_{0.3}MoO_3$, and $Rb_{0.3}MoO_3$. It was observed later that switching could be induced in $NbSe_3$ by doping with Fe, or by quenching [5], and that freshly grown samples displayed switching while aged crystals did not. Based on these observations, switching in $NbSe_3$ has been associated with the presence of "ultrastrong" pinning centers. At lower temperatures, two threshold fields, the lower one nonswitching and the upper one switching, have been observed in semiconducting materials such as $K_{0.3}MoO_3$, and also in $NbSe_3$ in the presence of a magnetic field [6]. The hysteresis increases as the temperature is lowered.

There have been a multitude of explanations for switching behavior [4]. Based on the importance of ultrastrong pinning centers, several models of switching have been proposed in which the dynamics of the CDW amplitude, ignored in the FLR model, is considered [7,8]. The role of normal carriers is also ignored in most treatments of CDW dynamics. Tucker *et al.* showed that normal carriers determine the time scale of dielectric relaxations of the pinned CDW [9]. Littlewood, elaborating on a two-fluid model of Sneddon [10], suggested that the inclusion of normal carriers could lead to two threshold fields and bistability of the CDW velocity, as observed in the semiconducting materials [11]. It was believed that the inclusion of normal carriers did not alter the form of the original FLR equations of motion, except to change the effective damping [10,12].

In this Letter, we show that when the effects of normal carriers are properly incorporated into the FLR model, we obtain an additional new global coupling term. Nonswitching behavior occurs in the limit of very weak pinning or small normal-carrier resistance. Switching occurs in the limits of strong pinning or large normal-carrier resistance. Both limits are consistent with experiment. We show how this model can be understood intuitively in terms of an electrical circuit. Numerical simulations in one dimension have been performed, consistent with our analytical results.

In the one-dimensional FLR model, the charge density is written as

$$\rho(x)=\rho_c+\rho_0\cos[Qx+\phi(x,t)],\quad Q=2k_F,$$

where ρ_c is the condensate density, ρ_0 is the CDW amplitude (held fixed), $\phi(x,t)$ is the CDW phase, and k_F is the Fermi wave vector. The CDW current is given by $j_{\rm CDW}(x,t)=-(e/\pi)\dot{\phi}(x,t)$. Ignoring inertial effects, the FLR equation of motion is

$$\gamma_0\dot{\phi}(x,t)=K\nabla^2\phi-\rho_0\sum_{i=1}^{N}V(x-x_i)\sin[Qx+\phi(x,t)]-(e/\pi)E(x,t), \tag{1}$$

where γ_0 is the CDW damping constant, K is the CDW elasticity, $V(x-x_i)$ is the potential due to an impurity at site x_i, N is the number of impurities, and $E(x,t)$ is the local electric field. At finite temperature, normal carriers are excited across the Peierls gap, leading to a linear conductivity σ with an Arrhenius temperature dependence. The total current in the presence of a spatially uniform external field E_0 (ignoring for simplicity displacement currents) is

$$j(x,t)=j_{\rm CDW}(x,t)+j_N(x,t)=-(e/\pi)\dot{\phi}(x,t)+\sigma E(x,t). \tag{2}$$

Incompressibility and current conservation ($\nabla\cdot\mathbf{j}=0$)

[13,14] yield

$$j_{CDW}(x,t)+j_N(x,t)=\langle j_{CDW}\rangle_x+\langle j_N\rangle_x ,$$

where $\langle\ \rangle_x$ denotes a spatial average. Solving for $E(x,t)$, one obtains

$$E(x,t)=E_0-(e/\pi\sigma)[\langle\dot{\phi}(x,t)\rangle_x-\dot{\phi}] . \quad (3)$$

The equations of motion can be written in a discretized form easily suited to numerical simulation by taking $V(r)=V_0\delta(x-x_i)$ and integrating out between impurities,

$$(\gamma_0+\gamma_1)\dot{\phi}_i=K\nabla^2\phi_i+W\sin(\phi_i-\beta_i)+V+\gamma_1\langle\dot{\phi}_i\rangle_i , \quad (4)$$

where ϕ_i represents the CDW phase at impurity site i, $\gamma_1=e^2/\pi^2\sigma$ is the Ohmic damping constant, L is the average distance between impurities [15], $\nabla^2\phi_i\equiv(\phi_{i+1}-2\phi_i+\phi_{i-1})/L$, $W\equiv-\rho_0V_0/L$, $V\equiv-eE_0/\pi$, $\beta_i\equiv Qx_i$ is a random variable mod2π, and $\langle\ \rangle_i$ denotes an average over impurity sites $i=1,2,\ldots,N$ [16]. We will henceforth work in units where $W=L=1$. Viewed in the reference frame of the moving CDW [11,17], the global coupling term $\gamma_1\langle\dot{\phi}_i(t)\rangle_i$ is by definition zero. But the CDW moving frame is not an inertial one; hence there will be a "fictitious" force $\gamma_i\langle\dot{\phi}_i(t)\rangle_i$. It is for this reason that we work in the inertial reference frame of the underlying lattice.

While the discretized version of Eq. (1) in the absence of normal carriers is often depicted in terms of balls and springs on a washboard, it also has a representation as an electrical circuit, as is shown in Fig. 1(a) for $N=3$. The impurity potential seen by the CDW is represented by a nonlinear capacitor, which has the Q-V relation $V=\sin(\phi_i-\beta_i)$, where ϕ_i represents the charge on the ith nonlinear capacitor. The domains are coupled by capacitors with capacitance $C=K^{-1}$, and are biased with a constant voltage V. The total CDW current is equal to the average of the currents through each nonlinear capacitor.

Figure 1(a) demonstrates some of the unphysical aspects of the FLR model in the absence of normal carriers. Experimentally, one cannot specify the voltage across each single domain, nor can one measure the current at each domain. Rather, one specifies the voltage across the entire sample, and measures the current, or vice versa. Also, it is impossible to perform current-driven numerical simulations of the FLR model, making it difficult to compare with many experiments. Such difficulties are remedied by including normal carriers. Figure 1(b) shows a circuit representation of Eq. (4). The voltage sources are replaced by resistors [18] with resistance γ_1, and the voltage across the ends of the network is NV (here, $N=3$). The arrow indicates how a local distortion of the CDW is compensated by a backflow of normal carriers. The circuit in Fig. 1(b) reduces to that in Fig. 1(a) if one lets γ_1 approach zero while holding V fixed (although the normal current becomes infinite).

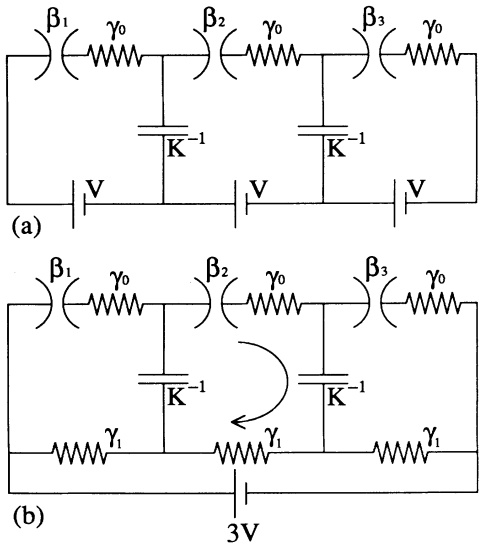

FIG. 1. (a) Circuit representation of Fukuyama-Lee-Rice model with $N=3$ impurities (see text for discussion). The impurity potential seen by the CDW is modeled by a nonlinear capacitor with $V=\sin(\phi_i-\beta_i)$, where ϕ_i is the charge on the ith capacitor. The total CDW current is $\langle\dot{\phi}_i(t)\rangle_i$. (b) Circuit representation of Eq. (4). The voltage sources are replaced by resistors, and a voltage NV is applied across the ends of the circuit. The arrow indicates how a local CDW current is compensated by a backflow of normal electrons, thus conserving the total current. This circuit reduces to that in (a) in the limit $\gamma_1\to 0$.

One of the consequences of the additional term in Eq. (4) is switching behavior. The global nature of the coupling term $\langle\dot{\phi}\rangle_i$ acts like an effective field which can "bootstrap" the CDW into a high-conduction state at a threshold field V_{t2}. The physical origin of the global coupling can be seen by imagining a situation where the CDW is pinned and V is close to V_{t2}. A local current flow, as indicated by the arrow in Fig. 1(b), will cause the voltage to drop across the center domain, thereby increasing the voltage across all the other domains. This situation is unstable for sufficiently large $\alpha\equiv\gamma_i/\gamma_0$, and can cause the CDW to switch to a high-conduction state. Once in the conducting state, the CDW can continue to slide until the voltage is lowered to $V_{t1}<V_{t2}$. We have performed numerical simulations of Eq. (4) for various values of α and K in a system with $N=50$ impurities. Figures 2(a) and 2(b) plot the time-averaged CDW current $\bar{J}_{CDW}$ vs V for various values of α and K. Figure 2(a) shows that V_{t2} is independent of α, while Fig. 2(b) shows that V_{t1} is insensitive to K, provided V_{t1} is sufficiently smaller than V_{t2}.

Figure 3 shows how the size of the hysteresis loop $(V_{t2}-V_{t1})/V_{t1}$ varies with α and K. In the strong-pinning regime, the hysteresis is immeasurably small until $\alpha\sim 1$. In the weak-pinning regime, the crossover to significant hysteresis occurs at a larger value of α, and is a decreasing function of K for fixed α.

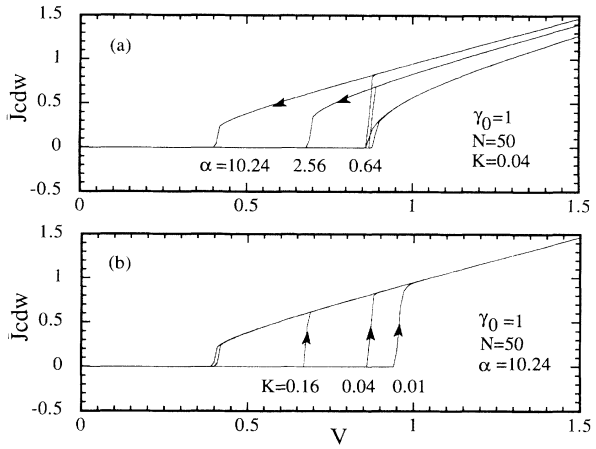

FIG. 2. (a) Plot of time-averaged CDW current $\bar{J}_{\rm CDW}$ vs V for various values of α and $K=0.04$ (see text for discussion). The upper threshold V_{t2} is independent of α. (b) Plot of I-V curves for various values of K and $\alpha=10.24$. The lower threshold V_{t1} is independent of K for V_{t1} sufficiently smaller than V_{t2}.

Much of the previous analysis of the FLR model carries over to Eq. (4), provided the system is in a particular pinned state. The reason is simple: In a stable pinned configuration, $\gamma_1\langle\dot{\phi}_i\rangle_i=0$, and hence, the location of the singular points in phase space will be independent of α. So, for example, the FLR arguments concerning the dependence on the upper threshold field V_{t2} on K for $\alpha=0$ remain valid for $\alpha>0$. For $K\ll 1$ (strong pinning), the threshold field $V_{t2}\approx 1$, while for $K\gg 1$ (weak pinning), $V_{t2}\propto K^{4/(d-4)}$ in d dimensions [2,3]. Figure 2(a) shows that V_{t2} is indeed independent of α [19] and Fig. 2(b) indicates that V_{t2} has the correct dependence on K, even for large α. Once in the sliding state, the picture changes dramatically. Estimating V_{t1} requires some manipulation of Eq. (4). One can reexpress the global term by averaging both sides over the impurities i, obtaining

$$\gamma_0\langle\dot{\phi}_i\rangle_i=\langle\sin(\phi_i-\beta_i)\rangle_i+V \tag{5}$$

and hence,

$$\gamma_0\dot{\phi}_i=\frac{K\nabla^2\phi_i+\sin(\phi_i-\beta_i)+\alpha\langle\sin(\phi_i-\beta_i)\rangle_i}{1+\alpha}+V. \tag{6}$$

Equation (6) looks similar to Eq. (4), but now the global coupling term involves the spatial average of $\sin(\phi_i-\beta_i)$. The time- and space-averaged pinning force is related to the time-averaged CDW current $\bar{J}_{\rm CDW}$ by $\langle\sin(\phi_i-\beta_i)\rangle_{i,t}=\gamma_0\bar{J}_{\rm CDW}-V$. In the pinned state. $\langle\sin(\phi_i-\beta_i)\rangle_i=-V$, and $\langle\dot{\phi}_i\rangle_i=0$. In the high-field limit, $\langle\sin(\phi_i-\beta_i)\rangle_{i,t}\approx 0$ and $\gamma_0\langle\dot{\phi}_i\rangle_{i,t}\approx V$. The high-field limit occurs at smaller V for larger α, as can be seen from Fig. 2(a). The pinning potential is scaled by $1+\alpha$, so that $V_{t1}\propto(1+\alpha)^{-1}$ for $\alpha\gg 1$. In the limit $K\to\infty$, one can view Eq. (5) as an equation of motion for $\Phi(t)\equiv\langle\phi_i(t)\rangle_i=\phi_j(t)$, for all j. In the limit $\alpha\to\infty$, one also obtains Eq. (5) for $\Phi(t)=\phi_j(t)+c_j$, where $\{c_j\}$ are "frozen." Thus, at low temperatures, the CDW behaves as a rigid object [11].

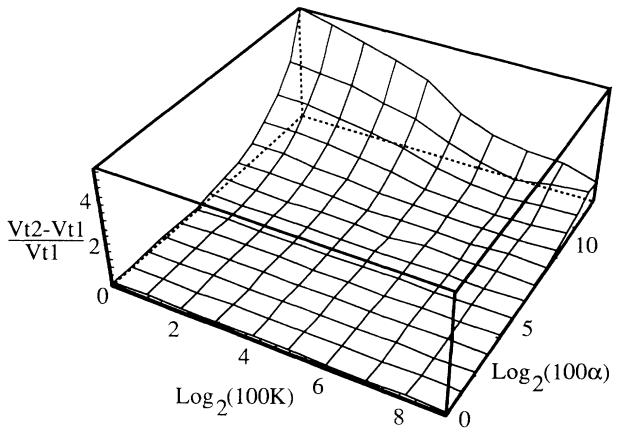

FIG. 3. Plot of hysteresis as a function of α and K, with $N=50$. Measurements were made at each grid intersection. Hysteresis for strong pinning begins near $\alpha=1$. For weak pinning, the onset of hysteresis occurs at a much larger value of α, and is smaller.

Switching behavior is the rule rather than the exception for the semiconducting CDW materials. As $T\to 0$, γ_0, dissipation arising from phason-phason and phason-phonon scattering [20], tends to zero, while γ_1 becomes exponentially large [14]. In terms of the circuit representation, this amounts to removing the bottom resistors and shorting the top ones, leading to a rigid CDW whose differential resistance becomes zero at threshold. Such behavior has in fact been observed in $K_{0.3}MoO_3$ and other semiconducting materials [21].

We believe that our model also accounts for switching behavior in $NbSe_3$, although the situation is complicated by the presence of a chain in the unit cell which remains metallic at low temperatures. The increase of the hysteresis loop width $V_{t2}-V_{t1}$ as temperature is lowered is consistent with increasing α at fixed K in our model. This is in apparent conflict with the fact that the normal resistance of $NbSe_3$ decreases as the temperature is lowered. This conflict suggests that the CDW is screened more effectively by quasiparticles on the CDW chain than by normal electrons on a neighboring chain, and that γ_1 cannot be simply assigned to the normal resistance in $NbSe_3$. We believe that the velocity discontinuities, or phase-slip centers, observed in switching samples of $NbSe_3$ are indicators of strong pinning centers but are not responsible for switching.

Another consequence of the global coupling term in Eq. (4) is the nonuniqueness of the sliding state. It has been shown that the FLR model obeys a so-called "no-crossing condition" [22], which requires the sliding state to be unique and the transition to the sliding state to be nonhysteretic. It is simple to show by construction that the global coupling term violates this no-crossing condi-

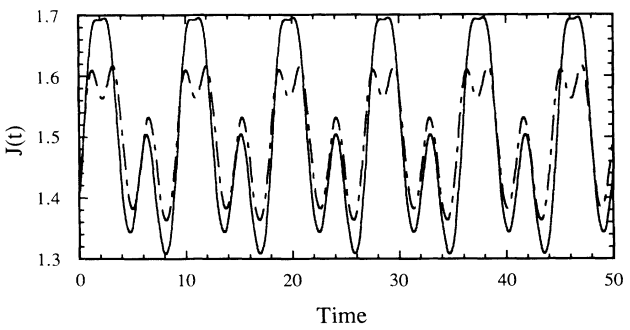

FIG. 4. Plot of steady-state total current $J(t)$ vs time for two different initial configurations and identical parameters $N=3$, $K=0.01$, $\gamma_0=1$, and $\alpha=1.28$. The total current $\bar{J}=1.490$ for the solid curve, and $\bar{J}=1.497$ for the dash-dotted curve.

tion, hence allowing multiple sliding states for a fixed voltage V. Such multiple sliding states are observed numerically for large N, and N as small as 3. Figure 4 shows the total current $J(t)$ versus time for two distinct sliding states corresponding to $V=1.0$ in a system with $N=3$. The magnitude of the current oscillations (narrow-band noise) are larger for the solid curve, but the time-averaged current is smaller. The effect of added noise might cause hopping between metastable running states, yielding long-term fluctuations of the narrow-band noise frequency, first noticed as such by Bhattacharya *et al.* [23].

The generalization of Eq. (4) to higher dimensions may yield two threshold fields, as observed experimentally. Also, observed differences between current- and voltage-driven experiments in switching samples may be borne out by analogous numerical "experiments." Other phenomena associated with switching [4], such as period doubling, negative differential resistance, and delayed switching, should be explored within the context of this model. Preliminary numerical experiments show that Eq. (4) exhibits period doubling, as well as delayed switching [24]. The global coupling term in Eq. (4) will very likely have a profound effect on the critical dynamics near threshold [25], even in parameter regimes where switching does not occur. This global coupling is present in many other nonlinear dynamical systems with many degrees of freedom, such as Josephson-junction arrays [26] and coupled laser systems [27], and its nonlinear dynamics should prove to be fascinating.

We gratefully acknowledge D. Scalapino and J. Carlson for many useful discussions, and A. Montakhab for a careful reading of the manuscript. This work was supported by the National Science Foundation DMR 8901651 (J.L., M.S.S.), the Alfred P. Sloan Foundation (M.S.S.), INCOR (J.L.), and the Office of Naval Research under Contract No. N00014-91-J-1257 (K.W.).

[a]Address until June 1992: Department of Physics, University of California at Santa Barbara, Santa Barbara, CA 93106-9530.

[1] For a recent review of the dynamics of sliding CDWs, see G. Grüner, Rev. Mod. Phys. **60**, 1129 (1988).
[2] H. Fukuyama and P. A. Lee, Phys. Rev. B **17**, 535 (1978).
[3] P. A. Lee and T. M. Rice, Phys. Rev. B **19**, 3870 (1979).
[4] For a review of the dynamics of switching CDWs, see R. P. Hall, M. F. Hundley, and A. Zettl, Phys. Rev. B **38**, 13002 (1988); R. P. Hall and A. Zettl, *ibid.* **38**, 13019 (1988); M. S. Sherwin, A. Zettl, and R. P. Hall, *ibid.* **38**, 13028 (1988), and references therein.
[5] K. Svoboda, A. Zettl, and M. S. Sherwin, Solid State Commun. **70**, 859 (1989).
[6] R. V. Coleman *et al.*, Synth. Met. **19**, 795 (1987).
[7] S. H. Strogatz, C. M. Marcus, R. M. Westervelt, and R. E. Mirollo, Phys. Rev. Lett. **61**, 2380 (1988).
[8] M. Inui, R. P. Hall, S. Doniach, and A. Zettl, Phys. Rev. B **38**, 13047 (1988).
[9] J. Tucker *et al.*, Phys. Rev. B **34**, 9038 (1986).
[10] L. Sneddon, Phys. Rev. B **29**, 719 (1984).
[11] P. B. Littlewood, Solid State Commun. **65**, 1347 (1988).
[12] P. B. Littlewood, in *Charge Density Waves in Solids,* edited by L. P. Gorkov and G. Grüner, Modern Problems in Condensed Matter Sciences Vol. 25 (North-Holland, Amsterdam, 1989), p. 321.
[13] W. L. McMillan, Phys. Rev. B **12**, 1197 (1975).
[14] L. Sneddon, Phys. Rev. B **29**, 719 (1984).
[15] One need not approximate the impurity distance by its average. See P. B. Littlewood, Phys. Rev. B **33**, 6694 (1986).
[16] Note that Eq. (3) follows directly from Eq. (2) when the condition $\nabla\cdot\mathbf{j}=0$ is satisfied.
[17] This approach was first taken by L. Sneddon, M. C. Cross, and D. S. Fisher, Phys. Rev. Lett. **49**, 292 (1982).
[18] One can model the effects of displacement currents by placing a capacitor in parallel with the normal resistor, and CDW inertia with an inductor in series with the CDW resistor.
[19] If the voltage is swept quickly, $\gamma_1\langle\dot{\phi}_i\rangle_i$ will not be zero, and hence V_{t2} will decrease. Such behavior is seen numerically, and has in fact been observed experimentally. See Y. M. Kim, G. Mihály, and G. Grüner, Solid State Commun. **55**, 663 (1989).
[20] S. Takada, K. Y. M. Wong, and T. Holstein, Phys. Rev. B **32**, 4639 (1985).
[21] G. Mihály and P. Beauchêne, Solid State Commun. **63**, 911 (1987).
[22] A. A. Middleton, Phys. Rev. Lett. **68**, 671 (1992).
[23] S. Bhattacharya, J. P. Stokes, M. J. Higgins, and R. A. Klemm, Phys. Rev. Lett. **59**, 1849 (1987).
[24] J. Levy and M. S. Sherwin (unpublished).
[25] D. S. Fisher, Phys. Rev. B **31**, 1396 (1985).
[26] P. Hadley, M. R. Beasley, and K. Wiesenfeld, Phys. Rev. B **38**, 8712 (1988); K. Wiesenfeld and P. Hadley, Phys. Rev. Lett. **62**, 1335 (1989).
[27] K. Wiesenfeld, C. Braicikowski, G. E. James, and R. Roy, Phys. Rev. Lett. **65**, 1749 (1990).